

Doping Effect on the Structural Properties of ZnO: Al₂O₃ Thin Films by Pulsed Laser Deposition

Ali A. Yousif*, Nadir F. Habubi* and Adawiya J.Haidar**

*Department of Physics, College of Education, University of Al-Mustansiriyah, Baghdad-Iraq.

**School of Applied Sciences, University of Technology, Baghdad-Iraq.

*E-mail: aliyousif73@gmail.com.

**E-mail:adawiya_haider@yahoo.com.

Abstract

Polycrystalline Alumina-doped Zinc Oxide (AZO) thin films on glass substrates have been deposited by pulsed laser deposition technique using pulsed Nd-YAG laser with wavelength ($\lambda=532$ nm) and duration (7ns). The structural properties of these films were characterized as a function of Al₂O₃ content (1 w.t%, 3 w.t% and 5 w.t %) in the target at substrate temperatures (200°C and 400°C) and energy fluence (0.4 J/cm²). The X-ray diffraction patterns and scanning electron microscopy (SEM) for the films showed that the undoped and Al₂O₃-doped ZnO films exhibit hexagonal wurtzite crystal structure and high polycrystalline quality with a preferred orientation along (100) plane. The grain size increases as the Al₂O₃ concentration increases to 85.6 nm. The surface morphology of the films obtained by scanning electron microscopy reveals that presence of Al₂O₃ content in the structure did affect the surface morphology of the films significantly.

Keywords: Al₂O₃ doped ZnO, Pulsed Laser Deposition (PLD), U.V emission, XRD.

1. Introduction

Zinc oxide has attracted attention as a transparent conducting oxide because of its (i) large band gap (3.3 eV), [1] (ii) high conductivity, (iii) ease in doping, (iv) chemical stability in hydrogen plasma, [2] (v) thermal stability when doped with III group elements, [3] and (vi) abundance in nature and nontoxicity. In addition to potential use as transparent conducting oxide in optoelectric devices, ZnO thin films also find application as gas sensors, [4] because of their high electrical resistivity. The optoelectric properties of ZnO thin films depend on the deposition and post deposition treatment conditions as these properties change significantly with (i) the nature of chosen doping element, (ii) the adsorption of oxygen that takes place during film deposition, (iii) film deposition temperature [5].

Several deposition techniques are used to grow aluminum-doped zinc oxide (AZO) thin films. These include chemical vapor deposition (CVD), [6] magnetron sputtering, [7] spray pyrolysis, [8,9] and pulsed laser deposition (PLD) [10,11]. In comparison with other techniques, PLD has many advantages such as

(i) the composition of the films grown by PLD is quite close to that of the target, (ii) the surface of the films is very smooth, (iii) good quality films can be deposited at room temperature due to high kinetic energies (>1 eV) of atoms and ionized species in the laser produced plasma. [12]

In this study, Al₂O₃-doped ZnO thin films were prepared using PLD on glass substrates at 200°C and 400°C temperature. We also investigated the influence of laser (0.4) J/cm² applied during the deposition process on the structural and morphological properties of the films.

2. Experiments Details

ZnO: Al₂O₃ thin films sintered target of high – purity 99.99% was mounted in a locally design vacuum chamber and ablated by a double frequency with Q- switched Nd: YAG pulsed laser operated at 532 nm, pulse duration of about 10 ns, and a (0.4) J/cm² energy density was focused on the target to generate plasma plume as shown in Fig. (1).

All samples were grown at optimal substrate temperature of 200°C and 400°C with oxygen background pressure of 2×10^{-2} mbar.

The morphological features of the various films were investigated with a JEOL JSM-6360 equipped with a EDAX detector. The SEM is used in its common mode, the emission mode. In this mode, electrons fired from a filament (tungsten hairpin or LaB6) are accelerated with a voltage in the range of 1-30 kV down the center of an electron-optical column consisting of two or three magnetic lenses. X-ray diffraction (XRD) measurements were performed by a Rigaku diffract meter with Cu K radiation ($\lambda = 1.5405 \text{ \AA}$).

3. Result and Discussion

3.1 Effect of Substrates Temperatures of Pure ZnO Films

The XRD pattern of pure ZnO target films show polycrystalline structure of hexagonal wurtzite phase as shown in Fig. (2) and (3), this shows the patterns of pure ZnO at different temperatures (200°C and 400°C). The films exhibit a dominant peak on $2\theta = 31.7^\circ$ corresponding to the (100) plane of ZnO at 200°C and peak on $2\theta = 31.748^\circ$ at 400°C, and other peaks corresponding to (002) and (101) and indicating the polycrystalline nature of the films. The intensity of XRD peaks is related to many factors, which include crystallization quality, density, and thickness of thin films, and so on. The intensities of ZnO (100) peaks in XRD spectra are different due to the diverse crystallization quality and various substrate temperatures in spite of the same deposition condition [13].

We can see that the film quality improved with the increase of the temperature. This is because the atoms at lower temperatures do not have enough energy to locate their right position [14]. It is seen from the figure that the relative intensity of the (100) peak increases with increasing temperature. The increase in peak intensity indicates an improvement in the polycrystalline of the films with increase in grain size [15].

3.2 Effect of Doping on Pure ZnO Films

Fig.(4) illustrates the XRD patterns of ZnO films with various Al_2O_3 doping concentrations. All the films exhibit the preferred (100) orientation due to the minimal surface energy in the ZnO hexagonal wurtzite structure [16]. No diffraction peaks of Al_2O_3 or

other impurity phases are found in these samples. The intensity of the (100) peaks increase with increasing Al_2O_3 -doping. In addition, the location of the (100) peaks was shifted to higher 2θ angles, from $2\theta = 31.7^\circ$ to $2\theta = 31.76^\circ$ as Al_2O_3 -doped content increases from 0 to 5 wt.%.

To compare our results with those given in the (ASTM data card 5-0664), one could conclude that the deposition films show a hexagonal structure of ZnO. Significant changes, observed in the X-ray diffraction patterns, manifest themselves in increase of peak intensity corresponding to (100) crystal plane and a decrease in the peak intensity corresponding to other planes.

The lattice constants and the relative intensity ratio, (100) in the diffraction pattern of undoped ZnO films deposited under various doping concentration are given in Table (1). The lattice constants obtained are found to be in good agreement with ASTM data 5-0664 powder ZnO sample.

The results of the (FWHM) for all samples point that they have values close together for undoped ZnO, $\text{ZnO}:\text{Al}_2\text{O}_3$ thin films of various doping concentration and increase for higher temperature for undoped ZnO. For Al_2O_3 concentration was found to be increase respectively as in Table (2).

The average grain size was calculated using Scherrer's formula equation (1), the values of average grain size listed in the Table (2) show a decrease with at higher temperature for undoped ZnO, and a decreased when the concentration of Al_2O_3 was increased at doped rate (1 at.%- 5 at.%). as shown in Table (2). [17]

$$g = \frac{(0.94\lambda)}{[\Delta_{(2\theta)} \cos \theta]} \dots\dots\dots (1)$$

Where:

λ : is the x-ray wavelength (\AA). $\Delta_{(2\theta)}$: FWHM (radian).

θ : Bragg diffraction angle of the XRD peak (degree).

The integral breadth of the samples were obtained from the XRD pattern sheets using the relation (2), our results indicate that β increase at higher temperature for undoped ZnO and increased for doping concentration

for Al₂O₃, the value of β were shown in Table (2). [18]

$$\beta = \frac{\text{Area}}{I_o} \dots\dots\dots(2)$$

Where:

Area = area under peak.

I_o = maximum intensity.

The shape factor was calculated using the relation (3), the results show that the shape factor decreased with increasing temperature for pure ZnO and doped in all concentration rates. [18]

$$\Phi = \frac{\Delta}{\beta} \dots\dots\dots(3)$$

The microstrain depends directly on the lattice constant (c) [19], and its value related to the shift from the ASTM standard value which could be calculated using the relation (1). No important effect of undoped ZnO and various doping concentration for alumina were recorded on the c-parameter, as seen in Table (2).

The residual stress with decreasing the temperature increases for pure ZnO and for all the doping concentration. The values of the residual stress for undoped ZnO, ZnO:Al₂O₃ thin films were given in Table (2). The stress is negative, so the biaxial stress is compressive [20].

Texture coefficient (T_c) of fabricated ZnO thin film was calculated using relation (4). The results indicate that (T_c) decrease with increasing doping for Al₂O₃ concentration. This is a consonantal result because increased doping causes an increase in the surface roughness. This result is in a good agreement with that in the Joseph [21].

$$TC(hkl) = \frac{[I(hkl)/I_o(hkl)]}{[Nr - 1 \sum I(hkl)/I_o(hkl)]} \dots\dots\dots(4)$$

Where:

I : is the measured intensity .

I_o : the ASTM standard intensity .

Nr : the reflection number .

(hkl) : Miller indices

4. Surface Morphology by (SEM)

4.1 Effect Doping Concentration

Figs. (5) (a, b, c and d) shows the surface images of ZnO films with various Al₂O₃ doping concentrations respectively, the films

were prepared on glass substrates using 0.4 J/cm² laser energy density 10⁻¹ mbar Oxygen pressure and 400°C substrates temperature. Were a significantly change in the morphology and structure of ZnO film after the Al₂O₃ doping. It has been found that the grain size increases as the Al₂O₃ concentration increases. The average grain sizes of the films with Al₂O₃ of 0 wt. %, 1 wt. %, 3 wt. % and 5 wt.% are 44, 70, 95, and 85.6 nm, respectively. The grains become densely packed near regularly. The average grain size δ deduced from x-ray diffraction using the Scherrer's formula is estimated at ~ (33- 69) nm. Therefore, as shown in SEM surface micrograph the grain size is larger than that estimated from XRD data [22]. See Table (3).

5. Conclusions

ZnO: Al₂O₃ thin films were deposited on glass substrate by Pulsed Laser Deposition at 200°C and 400°C temperature and at 10⁻² mbar oxygen background gas. The structural properties are found to be dependent on the laser energy density and temperature. The XRD studies indicate that the deposited of pure ZnO and ZnO:Al₂O₃ Films on glass substrate are polycrystalline and grown in the hexagonal phases wurtzite structure and high preferential orientation in (100) plane for different temperature and laser energy density. The average grain size for (100) plane increases with increase in dopant concentrations Al₂O₃ Films. The SEM average grain size increase with increase in dopant concentrations Al₂O₃ Films and increase in the of pure ZnO films.



Fig. (1) Pulsed laser deposition (PLD) system.

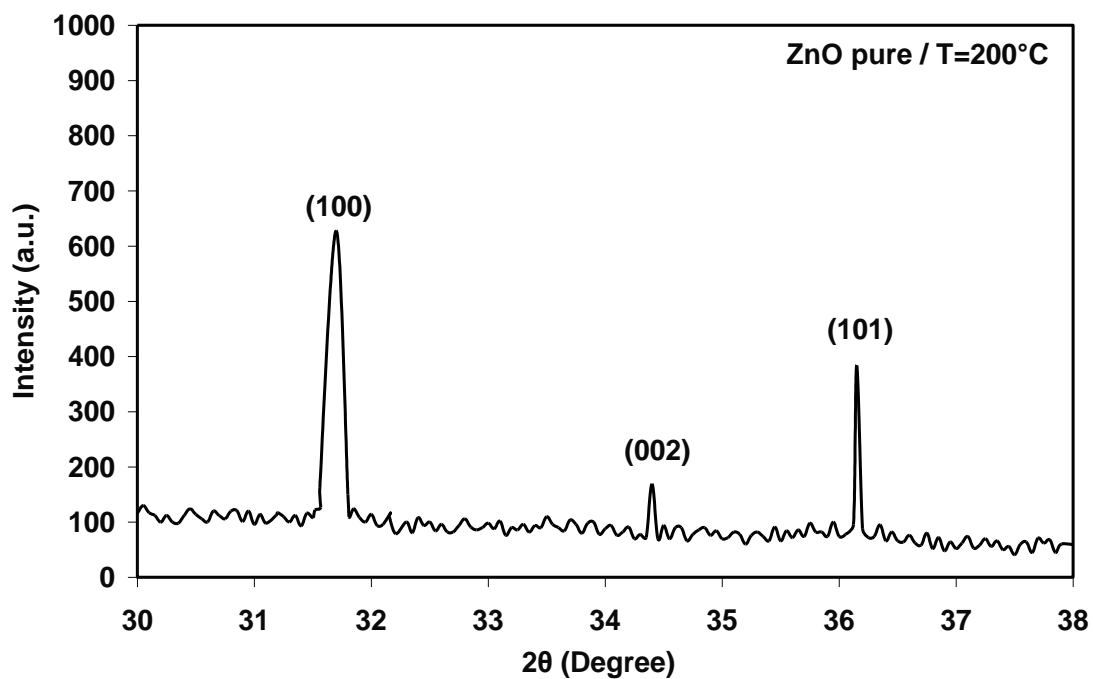


Fig. (2) XRD patterns of pure ZnO films grown on glass substrates at temperature 200°C.

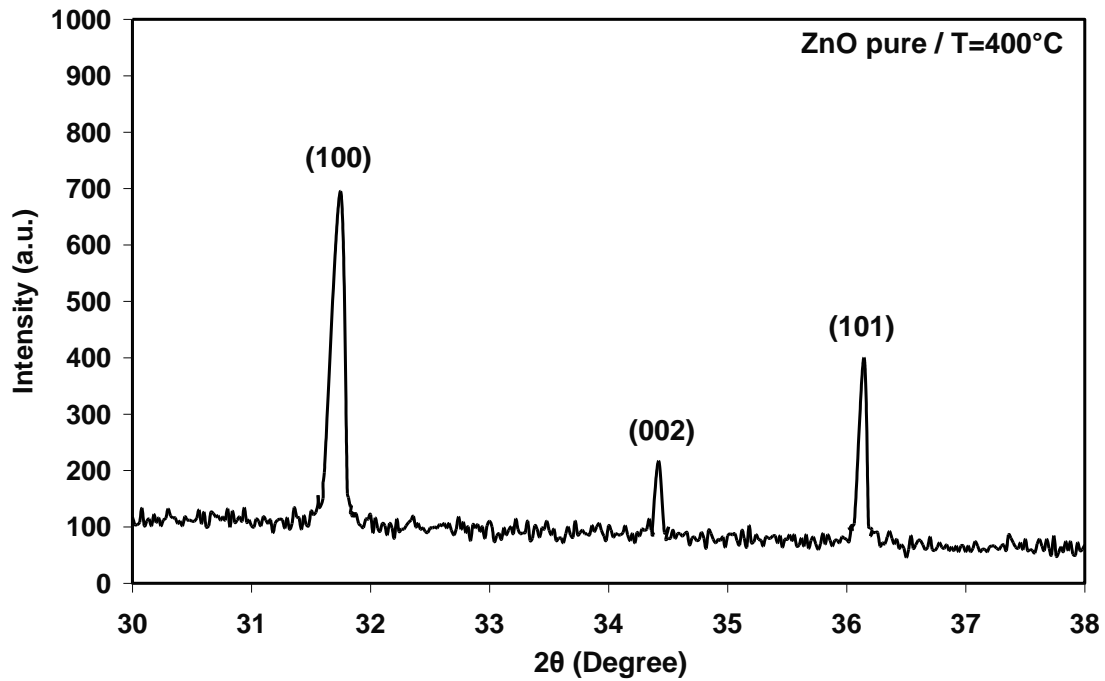


Fig. (3) XRD patterns of pure ZnO films grown on glass substrates at temperature 400 C.

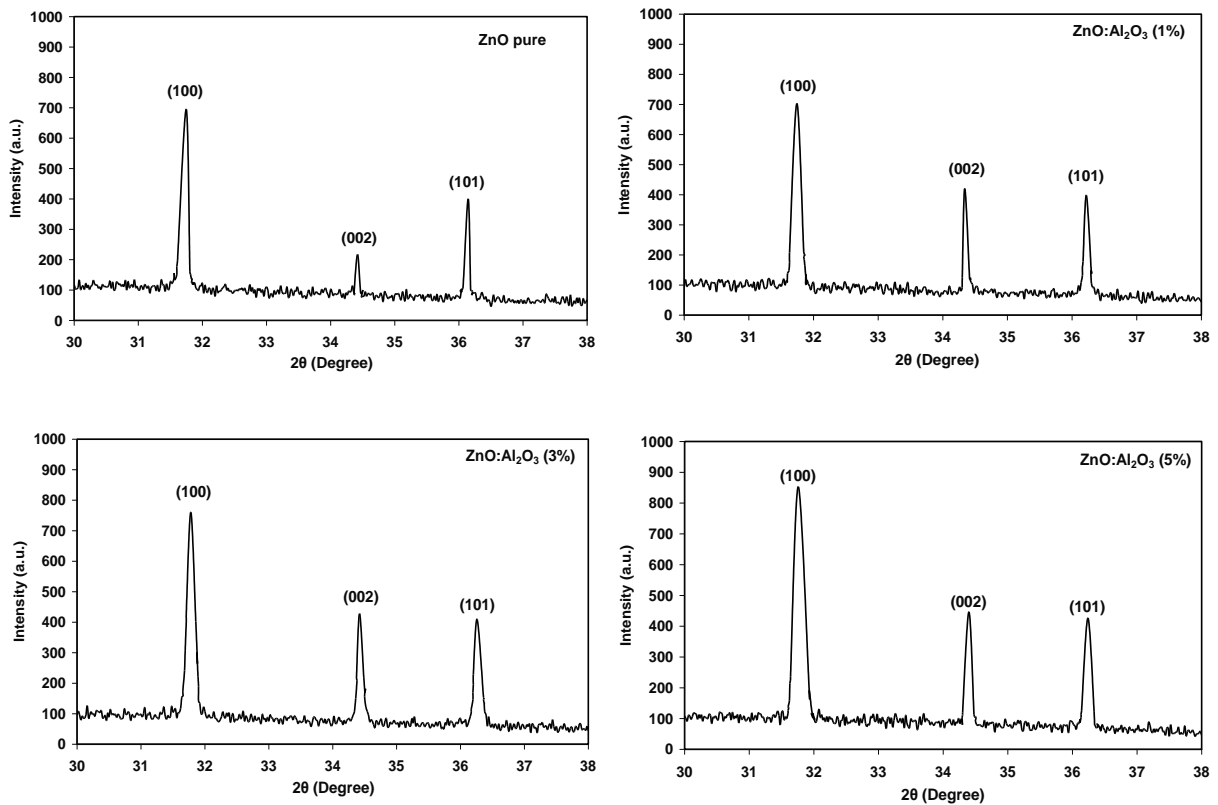


Fig. (4) XRD spectrum of ZnO pure and alumina-doped ZnO thin films Deposited on glass substrate.

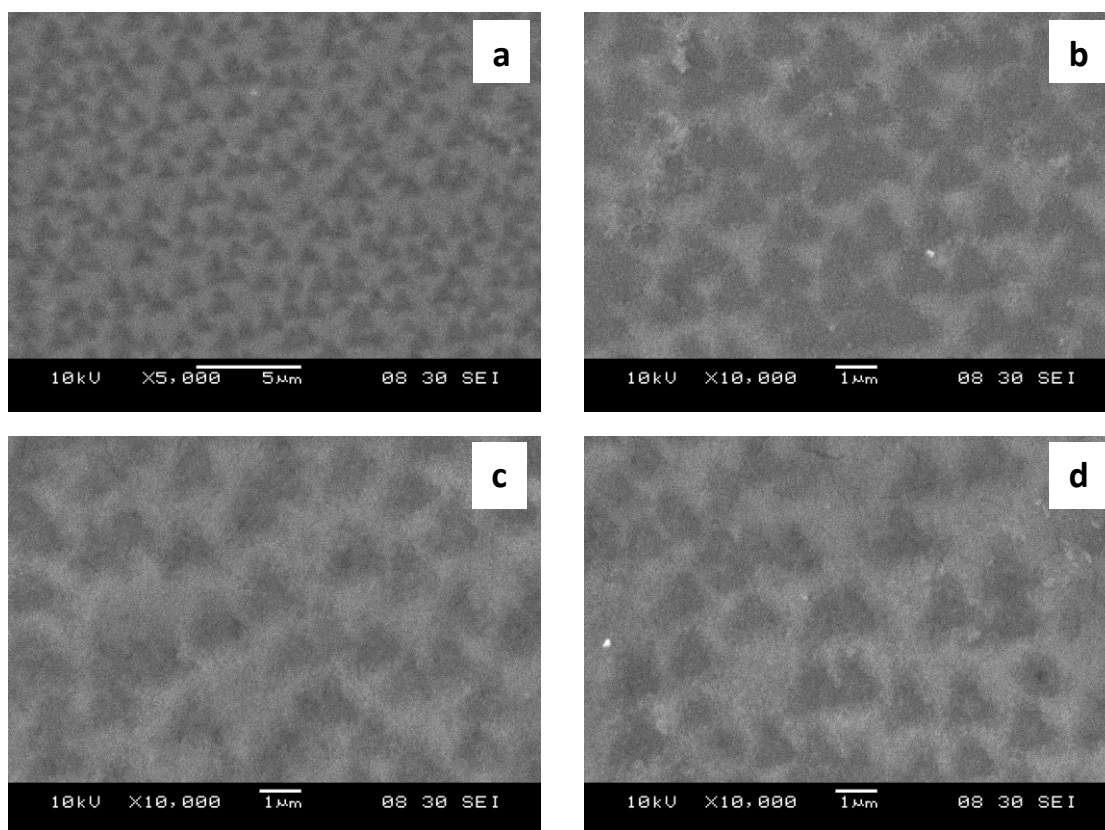


Fig. (5) SEM images for pure ZnO and Al₂O₃-doped ZnO thin films thin films (a) undoped, (b) 1 at.% Al₂O₃, (c) 3 at.% Al₂O₃ and (d) 5 at.% Al₂O₃.

Table (1)

Lattice constants and interplanar spacing as a function of undoped ZnO, ZnO:Al₂O₃ and ZnO:Co thin films of various doping concentration.

Sample	Investigated line	2θ	θ	$d \text{ \AA}$	$a_c \text{ \AA}$	$c_c \text{ \AA}$
ASTM	100	*	*	2.816	3.249	5.205
ZnO-pure T=200°C	100	31.7	15.85	2.812	3.247	5.234
ZnO-pure T=400°C	100	31.748	15.87	2.813	3.248	5.300
ZnO:Al ₂ O ₃ (1%) T=400°C	100	31.74	15.87	2.813	3.248	5.212
ZnO:Al ₂ O ₃ (3%) T=400°C	100	31.78	15.89	2.822	3.258	5.205
ZnO:Al ₂ O ₃ (5%) T=400°C	100	31.76	15.88	2.822	3.258	5.089

Table (2)
The Size – strain data of investigated thin films.

Sample	Investigated line	FWHM (deg)	Grain size g.s (nm)	Integral breadth β	Shape factor Φ	Strain δ (%)	Stress σ	Texture Coefficient T_C (h k l)
ZnO-pure T=200°C	100	0.270	30.8	0.131	2.06	9.122	-0.0804	1.7
ZnO-pure T=400°C	100	0.254	32.7	0.190	1.33	9.167	-0.0808	1.68
ZnO:Al ₂ O ₃ (1%) T=400°C	100	0.138	60.3	0.199	0.693	9.167	-0.0808	1.4
ZnO:Al ₂ O ₃ (3%) T=400°C	100	0.119	69.79	0.198	0.601	9.564	-0.0843	1.44
ZnO:Al ₂ O ₃ (5%) T=400°C	100	0.135	61.55	0.242	0.557	9.564	-0.0843	1.5

Table (3)
Structural and morphological characteristics of the ZnO (undoped and Al₂O₃ doped) films deposited at 400 °C substrate temperature 0.4 J/cm² leaser energy and 10⁻¹ mbar Oxygen pressure.

Sample	x-ray of plane grain size [nm]	SEM of plane grain size [nm]
ZnO-pure	33	44
ZnO:Al ₂ O ₃ (1%)	60	70
ZnO:Al ₂ O ₃ (3%)	70	95
ZnO:Al ₂ O ₃ (5%)	62	86

References

- [1] Malik, A., Seco, A., Nunes, R. *Flat Panel Display Materials III, Mrs Proc.*, Materials Research Vieira, M., Fortunato, E. Society, Vol. 471, p. 47, (1999).
- [2] Shanti, E., Banerjee A., and *Thin Solid Films*, (1983), 108, P. 333.
- [3] Tansley, T. L., Neely, D. F. and *Thin Solid Films*, (1984), 117, 19.
- [4] Khranovskyy et al., *Thin Solid Films* 517 (2009) 2073–2078.
- [5] Nunes, P. *et al. Vacuum*, (1999), 52, 45.
- [6] J. HU and Gordon, R. G. *J. Appl. Phys.*, (1992), 71, 880.
- [7] Igasaki, Y. and Saito, H. *J. Appl. Phys.* (1991), 70, 3613.
- [8] Aktaruzzaman, A. F., Sharma, G. L. *Thin Solid Films*, (1991), 198, 67. and Malhotra, L. K.
- [9] Goyal, D., Solanki, P., Maranthe, Takwale, M. and Bhide, V B., *Jap. J. Appl. Phys. 1*, (1992), 31, 361.
- [10] Suzuki, A., Matsushita, T., Wada, Sakamoto, Y. and Okuda, M. N., *Jap. J. Appl. Phys. 2*, (1996), 35, L56.
- [11] Hiramatsu, M., Imaeda, K., Horio, Nawata, M. N. *J. Vac. Sci. Technol. A*, (1998), 16, 669.

- [12] Chrisey, B. D. and Hubler, G. K. *Pulsed laser deposition of thin films*, Wiley, (1994).
- [13] F. K. Shan, B. C. Shin, S.W. Jang, Y. S. Yu, " *Substrate Effect of ZnO Thin Films Prepared by PLD Technique*", J. of the Eur. Cer. Soc. 24 (2004), P. 1015.
- [14] Wang Zhao-yang, Hu Li-zhong, Zhao Jie, Sun Jie and Wang Zhi-jun, " *Vacuum*", V.78 (2005) PP. 53-57.
- [15] P. Sagar, M. Kumar and R. M. Mehra, " *Materials Science-Poland*", V. 23, N. 3, (2005) P. 685.
- [16] J.F. Chang, H.L. Wang, M.H. Hon and Journal of Crystal Growth, V. 211 (2000) P. 93.
- [17] C. Gümüs , O.M.Ozkendir , H. Kavak , and Y. Ufuktepe , " *J. Optoelectronics and Advanced Mater.* ", 8, 1, (2006), PP. 299-303.
- [18] P. Šutta, and Q. Jackuliak , " *Mater. Struct.*", 5, 1, (1998), PP. 10-14.
- [19] T. Obata , K. Komeda , T. Nakao , H. Ueba , and C. Tasygama , " *J. Appl. Phys.* " , 81 , (1997) , 199 .
- [20] C. Li, X.C. Li, P.X. Yan, E.M. Chong, Y. Liu, G.H. Yue, X.Y. Fan, Appl. Surf. Sci., V. 253 (2007) P. 4000.
- [21] B. Joseph, P.K.Manoj , and V.K.Vaidyan , Bull. Mater. Sci., V.28 , N. 5 (2005) pp. (487-493).
- [22] D R Patil, L A Patil and D. P Amalnerkar Bull. Mater. Sci., V. 30, No. 6, December (2007), pp. 553–559.

المجهر الالكتروني (SEM) بالنسبة للاغشية الغير المشويه والمشويه بأنها ذات تركيب سداسي متعدد التبلور وبتجاه مفضل على طول المستوي (100). ان حجم الحبيبات يزداد بزيادة تركيز الالومينا الى (85.6 نانومتر). ان التركيب السطحي الذي حصلنا عليه من فحص المجهر الالكتروني بالنسبة للاغشية المشوب الالومينا كان له تأثير على تركيب الاغشية بشكل واضح.

الخلاصة

في هذا البحث، تم ترسيب أغشية اوكسيد الزنك المشوب بالالومينا (AZO) ذو تركيب متعدد البلورات ، تم ترسيبها على قواعد من الزجاج باستخدام تقنية ترسيب بالليزر النبضي، حيث استخدام ليزر النيديميوم- ياك عند الطول الموجي (532 نانومتر) و آمد نبضة (7 نانو ثانية). تم دراسة الخصائص التركيبية كدالة لتركيز الالومينا بنسب (1 %، 3 % و 5 %) في الهدف عند درجة حرارة القاعدة (200°C and 400°C) وكثافة طاقة الليزر الساقطة (0.4 J/cm²). اظهرت نتائج حيود الاشعة السينية وفحص